



ELSEVIER

Biochimica et Biophysica Acta 1408 (1998) 180–202

BIOCHIMICA ET BIOPHYSICA ACTA

BBA

Review

Formation and structure of surface films: captive bubble surfactometry

Samuel Schürch ^{a,*}, Francis H.Y. Green ^b, Hans Bachofen ^c^a *Respiratory Research Group, Department of Physiology and Biophysics, University of Calgary, Health Sciences Centre, 3330 Hospital Drive N.W., Calgary, Alta. T2N 4N1, Canada*^b *Respiratory Research Group, Department of Pathology, University of Calgary, Health Sciences Centre, Calgary, Alberta T2N 4N1, Canada*^c *Department of Internal Medicine and Institute of Anatomy, University of Berne, CH-3010 Berne, Switzerland*

Received 6 May 1998; received in revised form 19 June 1998; accepted 19 June 1998

Abstract

The adsorption model for soluble surfactants has been modified for suspensions of pulmonary surfactant. The dynamic adsorption behavior may be governed by a two-step process: (1) the transfer of molecules between the surface layer and the subsurface layer, which has a thickness of a few molecular diameters only; (2) the exchange of molecules between the subsurface and the bulk solution. The first step is an adsorption process and the second step is a mass transfer process. Between the subsurface and the bulk solution is an undisturbed boundary layer where mass transport occurs by diffusion only. The thickness of this boundary layer may be reduced by stirring. Rapid film formation by adsorption bursts from lipid extract surfactants, as observed in the captive bubble system, suggests that the adsorption process as defined above is accompanied by a relatively large negative change in the free energy. This reduction in the free energy is provided by a configurational change in the association of the specific surfactant proteins and the surfactant lipids during adsorption. The negative change in the free energy during film formation more than compensates for the energy barrier related to the film surface pressure. In the traditional view, the extracellular alveolar lining layer is composed of two parts, an aqueous subphase and a surfactant film, believed to be a monolayer, at the air–water interface. The existence and continuity of the aqueous subphase has recently been demonstrated by Bastacky and coworkers, and a continuous polymorphous film has recently been shown by Bachofen and his associates, using perfusion fixation of rabbit lungs with slight edema. In the present chapter, we have described a fixation technique using a non-aqueous fixation medium of perfluorocarbon and osmium tetroxide to fix the peripheral airspaces of guinea pig lungs. A continuous osmiophilic film which covers the entire alveolar surface, including the pores of Kohn, is demonstrated. By transmission electron microscopy, the surface film frequently appears multilaminated, not only in the alveolar corners or crevices, but also at the thin air–blood barrier above the capillaries. Disk-like structures or multilamellar vesicles appear partially integrated into the planar multilayered film. In corners and crevices, tubular myelin appears closely associated with the surface film. Tubular myelin, however, is not necessary for the generation of a multilaminated film. This is demonstrated *in vitro* by the fixation for electron microscopy of a film formed from lipid extract surfactant on a captive bubble. Films formed from relatively high surfactant concentration (1 mg/ml of phospholipid) are of variable thickness and frequent multilayers are seen. In contrast, at 0.3 mg/ml, only an amorphous film can be visualized. Although near zero minimum surface tensions can be obtained for both surfactant concentrations, film compressibility and mechanical stability are substantially better at the higher concentrations. This appears to be related to the multilaminated structure of the film formed at the higher concentration. © 1998 Elsevier Science B.V. All rights reserved.

* Corresponding author. Fax: +1-403-270-8928; E-mail: schurch@acs.ucalgary.ca

Keywords: Adsorption; Energy barrier; Conformational change; Preferential adsorption; Surfactant reservoir; Monolayer; Multilayer

Contents

| | |
|---|-----|
| 1. Introduction | 181 |
| 2. Film formation | 182 |
| 2.1. Adsorption | 182 |
| 2.2. Adsorption kinetics | 183 |
| 3. Captive bubble studies | 185 |
| 3.1. Methods | 185 |
| 3.2. Measurements of adsorption | 185 |
| 3.3. Surface activity of surfactants | 186 |
| 4. The surface-associated surfactant reservoir | 190 |
| 4.1. Reservoir formation: the role of SP-B and SP-C | 190 |
| 5. Film structure | 193 |
| 5.1. Alveolar surface lining layer | 193 |
| 5.2. Multilayers at the alveolar surface | 194 |
| 5.3. Surface film in vitro: recent investigations | 195 |
| 6. The surfactant film: monolayer or multilayer? | 197 |
| 6.1. Film structure | 197 |
| 6.2. Film formation | 197 |
| 6.3. Monolayer hypothesis | 198 |
| 6.4. Monolayer approximation | 198 |
| 6.5. Surface tension: mechanical equilibrium | 198 |
| 6.6. Nonmonolayer properties | 199 |
| 7. Summary and future directions | 199 |
| 8. List of Symbols | 200 |
| Acknowledgements | 200 |
| References | 200 |

1. Introduction

At least three physical properties of the surfactant system are essential for normal lung function, especially in the neonatal period. These are (1) rapid film formation through adsorption from the hypophase, (2) low film compressibility with a fall in surface tension to very low values during surface compression, and (3) effective replenishment of the surface film as an expansion by the incorporation of surfactant material (including squeezed-out components) from material associated with the surface.

Studies related to the material associated with the surface have been conducted by depleting the subphase of surfactant after the initial (de novo) film formation at the air–water interface of a captive bubble and by replacing the subphase with a pure salt solution without disturbing the bubble. These experiments have demonstrated the presence of ‘surplus’ material in the air–liquid interface upon de novo adsorption of surfactant derived from natural sources [1]. In addition, depletion experiments have shown that if films are compressed beyond the point of collapse at minimum surface tension (overcom-

pression), a collapse phase is formed and remains associated with the surface active film. This collapse material associated with the air–liquid surface is in addition to the ‘surplus’ material found associated with the interface after *de novo* adsorption. The collapse material may be incorporated into the surface active film on surface extension during repeated dynamic cycling [2]. Thus, the adsorption at the air–liquid interface on bubble expansion during repeated dynamic cycling of surfactant films derived from natural sources may involve film formation by the adsorption of surfactant material from three compartments, from the bulk suspension, from the material associated with the surface formed by *de novo* adsorption, and from the collapse phase generated by overcompression at minimum surface tension.

As outlined by Pattle [3], the lining layer of surfactant should be composed of two parts: a monomolecular film of phospholipids, associated with some proteins, and the lining complex of saline-dispersible lipoprotein serving as a reserve material. This concept of a monomolecular film lining an aqueous subphase, containing surfactant structures, represents the well-accepted traditional view of the acellular lining complex, as deduced from physiological experiments and biochemical analysis [4].

Weibel and associates demonstrated for the first time by electron microscopy the existence of an extracellular duplex lining layer of lung alveoli [5]. These authors observed that parts of the surface film appears as a lamellar superficial layer with repeating distances of 3.8 to 5.1 nm adsorbed to the surface film. Grossmann and Robertson [6] also found the surfactant film to be multilamellar and so did Ueda et al. [7] in their ultrastructural studies on the alveolar lining layer, using a variety of fixation methods. However, the postulated continuity of the lining layer consisting of a surfactant monolayer and an aqueous subphase could not be proven by chemical fixation.

Recent experiments have been more successful in preserving and demonstrating the lining layer. Bastacky and associates [8] demonstrated the continuity of the aqueous subphase, and Bachofen and co-workers [9,10] demonstrated a continuous osmophilic film lifted off the epithelial cell layer by alveolar edema fluid generated by high-pressure perfusion of excised rabbit lungs. High-power magnification of

the film showed a polymorphous structure. At some sites, triple or even higher order multilayers covered the increased volume of the hypophase whereas other sites of the lining layer appeared amorphous.

These observations are in line with the concept of a surface-associated surfactant reservoir observed in experiments in which the subphase below the surfactant film of a captive bubble was replaced by a salt solution that contained no surfactant. In this chapter, we focus on the formation of the surface lining including the surface active film and the reserve material associated with the surface active film and on the morphology of this surface lining. We address the question of whether the surface-associated surfactant material acts as reserve material to be incorporated into the surface active film which might be considered a monolayer, without essentially modifying the mechanical properties of the monolayer, or whether the associated material is mechanically coupled with the monolayer such that the mechanical properties of the interfacial lining between the vapor and the liquid phase are different from those of a monolayer.

2. Film formation

2.1. Adsorption

Adsorption means the accumulation of material at an interface. The surface or interface represents a region of generally unknown thickness in which the concentration of each component somehow changes from the value it has in one phase, α , to the value it has in the other phase, β . Exact definitions of adsorption are based on Gibbs' pioneering work, and on later versions by Guggenheim [11–13]. A decrease in surface tension with an increase in the concentration of a particular solute in the surface phase means that the solute is positively adsorbed at the surface. Any substance leading to this surface tension decrease is said to be ‘surface active’ [11]. Adsorption of surfactant molecules from surfactant suspensions is usually assessed by measuring the decrease of surface tension, but adsorption might also be investigated by employing the Gibbs adsorption equation which, in its simplest form, gives the number of surfactant molecules adsorbed per unit area at the surface (the Gibbs dividing surface) if the relation be-

tween the bulk surfactant concentration and the surface tension by adsorption is known [11].

2.2. Adsorption kinetics

2.2.1. Transport mechanisms

When a new surface in a surfactant solution is created, a finite time is required to reach an equilibrium between the surface concentration (Γ) and the bulk concentration (C). The non-equilibrium surface tension is called dynamic surface tension [14]. The dynamic surface tension is a function of time and surface composition. For solutions of soluble surfactants, the dynamic adsorption behavior is governed by a two step process [14] (Figure 1): (1) the transfer of molecules between the interfacial layer and the subsurface layer, the layer immediately below the interfacial layer – the subsurface layer has a thickness of a few molecular diameters only; (2) the exchange of molecules between the subsurface and the bulk solution. The first step is an adsorption process and the second step is a bulk mass transfer process.

There are four major transport mechanisms: (1) diffusion, (2) thermal convection, (3) flow (convective transport) and (4) convective-diffusion processes (coupled transport). The adsorption from turbulent or stirred solutions incorporates coupled transport of

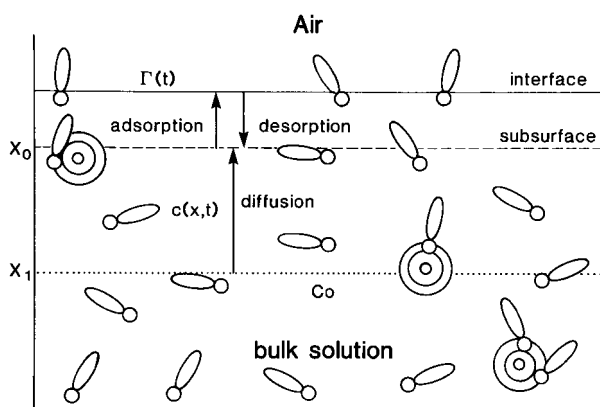


Fig. 1. A schematic diagram of the dynamic adsorption mechanism. Molecules adsorb from the subsurface layer, the layer immediately below the surface. The subsurface layer has a thickness of a few molecular diameters only. Diffusion proceeds from a diffusion length ($x_1 - x_0$), which is the thickness of the boundary layer. At longer times, desorption may also occur. Surfactant molecules may exchange with aggregates in solution. (Modified from Chang and Franses [14], with permission.)

solutes by a combination of convection and diffusion [15].

In diffusion-controlled adsorption models, in the absence of stirring, one assumes that there is no activation energy barrier to transfer the solute molecules between the subsurface (a few molecular diameters from the surface) and the surface. Thus, diffusion is the only mechanism needed to establish adsorption equilibrium (Fig. 1). The time required for the solute to transfer from the bulk to the subsurface is much longer than the time required for equilibration between the subsurface and the surface. This is the local equilibrium model, i.e., the surface concentration $\Gamma(t)$ is always at equilibrium with the subsurface concentration, $c(x_0, t)$ which changes as diffusion occurs. Hence,

$$\Gamma(t) = 2c_0(Dt/\pi)^{1/2} \left[1 - \frac{C_0(\pi D)^{1/2}}{2\Gamma_e} t^{1/2} + \dots \right] \quad (1)$$

where c_0 is the bulk surfactant concentration, D is the diffusion coefficient of the bulk phase, and Γ_e is the equilibrium surface concentration at concentration c_0 . Equation [1] only applies to small times, i.e., $\Gamma(t)$ is proportional to $t^{1/2}$ only at the initial stage of adsorption [14].

All fluid interfaces contain an undisturbed layer of solution adjacent to the interface. Mass transport in this boundary layer ($x_1 - x_0$) occurs only by diffusion (Fig. 1). The thickness of the boundary layer depends on temperature, stirring and the composition of the solution. It is up to 0.1 cm in unstirred systems and approaches 10^{-3} cm in well-stirred systems [15,16]. If the bulk solution is kept stirred to within a distance Δx of the subsurface, diffusion to the subsurface may be stationary. This is possible if new solute is continuously being brought to the lower limit of the layer Δx by convection and if back diffusion and depletion of the bulk solution can be neglected [16].

For the stationary case, the diffusion equation becomes:

$$\Gamma(t) = c_0 \frac{D}{\Delta x} t \quad (2)$$

The rate of adsorption at the surface is then inversely proportional to the thickness of the boundary layer, i.e., the rate of adsorption is increased by reducing Δx by stirring. In summary, the initial rate of adsorption may be diffusion controlled, and it is pro-

portional to $t^{-1/2}$; the later stage may become independent of time if the solution is well-stirred and if depletion of the solution is negligible. Then the rate of adsorption is inversely proportional to the thickness of the boundary layer and is controlled by diffusion across this boundary layer.

2.2.2. Energy barrier and conformational changes

Experiments on the adsorption of amphiphilic molecules and proteins may show a decrease in the rate of adsorption due to an energy barrier related to the energy needed for a molecule to clear an area ΔA against the surface pressure Π , $\Pi\Delta A$. In addition to this energy barrier, a molecule adsorbing at an interface having an electrical potential must do work against this electrical potential barrier [15]. Whereas the energy barriers tend to decrease the rate of adsorption to below that predicted by a diffusion-controlled process, the difference in the potential energy of the molecule in solution and when it is adsorbed at the interface might accelerate the adsorption.

Studies on protein adsorption have shown that adsorption is accompanied by protein unfolding and that the degree of unfolding at the air–water interface is related to the amino acid composition of the protein. The free energy of adsorption at the air–water interface appears determined by the nonpolar residues, such as Ala, Leu, Val, Met, Phe [12]. Not only the total amount of the nonpolar segments compared to that of the polar segments appears to be important for a particular protein to adsorb and unfold at the air–water interface, but also the distribution of the nonpolar segments among the polar segments through the protein chain is important. For example, in hemoglobin the adsorbing nonpolar segments are evenly distributed throughout the chain, thus giving complete unfolding with an area per residue of 0.17 nm^2 . In contrast, the cytochrome *c* molecule has relatively large patches of polar groups which give a very small potential energy in an aqueous solution and incomplete unfolding and limited adsorption at the air–water interface with an area per residue of 0.04 nm^2 [12].

The above concept is further supported by the calculation of the standard free energy of transfer from water to air for various amino acid residues and by the measurements of the standard free energy

of transfer for the same residues from water to oil [12]. For example, for the transfer of proline from water to air, ΔG was -30.0 kJ/mol and that for alanine was -9.2 kJ/mol . In addition, according to Traubes rule [11], the free energy of transfer for a CH_2 group from water to air is in the order of -2900 J/mol . This explains the fact that higher alcohols, e.g., hexadecanol, are strongly adsorbed at the water–air interface [17].

From the principles of statistical mechanics [18,19] it follows that the ratio of the number of particles, n_1 , in the higher state of potential energy E_1 , and the number, n_0 , in the lower state of energy, E_0 , is:

$$\frac{n_1}{n_0} = e^{-(E_1 - E_0)/kT} \quad (3)$$

where k is the Boltzmann constant and T is the absolute temperature.

Assuming the molecules arrive at the subsurface by diffusion, we can now estimate their initial rate of adsorption at the interface (Fig. 1):

$$\frac{d\Gamma}{dt} = c_0 \left(\frac{D}{\pi t}\right)^{1/2} e^{-(E_1 + \Pi\Delta A - E_0)/kT} \quad (4)$$

i.e., the probability that a number of molecules per unit time and unit surface are adsorbed at the interface is proportional to $\exp[-(E_1 + \Pi\Delta A - E_0)/kT]$ in thermal equilibrium.

Under the conditions that the pressure, temperature and number of molecules are constant, E_0 is the Gibbs free energy G_0 of the molecules in the subsurface and E_1 is G_1 , the Gibbs free energy of the molecules in the air–water interface. In Eq. 4, Π is taken as constant. However, Π is increasing as the area per molecule in the interface decreases, so $\Pi = \Pi(A)$ and $\Pi\Delta A$ has to be replaced by $\int_{A_1}^{A_2} \Pi(A) dA$.

If diffusion to the subsurface is assumed to be stationary due to convective transport by stirring, the diffusion term in Eq. 4 is replaced by $c(D/\Delta x)$; see Eq. 2. From Eq. 4 we see that if E_1 is smaller than E_0 , there is a thermodynamic driving force for the molecules to move to the interface. If E_1 is much smaller than E_0 , then the favorable free energy change in the adsorption process more than compensates for the energy barrier due to the surface pressure or other energy barriers, and the rate of adsorption is substantially increased.

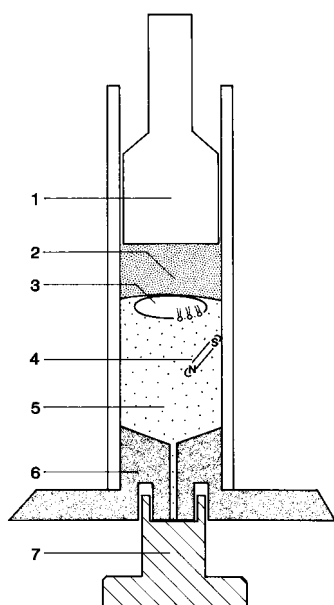


Fig. 2. The captive bubble surfactometer (CBS). (1) Pressure tight piston; (2) 1% agarose gel; (3) air bubble with surfactant on its air–liquid interface; (4) stir bar; (5) surfactant suspension in chamber; (6) stainless-steel base with inlet; (7) pressure tight plug. A bubble of atmospheric air 2–7 mm in diameter is drawn into the sample chamber to assume its resting position below the agarose gel. Bubble volume and, thus, bubble surface area is compressed or expanded by the changing pressure produced by the relative movement between piston and chamber. In the design of Putz and associates [25], the pressure changes are not driven directly with a piston, the bubble volume is regulated by an external pressure reservoir. Both approaches give equivalent results.

3. Captive bubble studies

3.1. Methods

The captive bubble surfactometer (CBS) (Fig. 2) introduced by Schürch and co-workers [20,21] offers a leak-proof system because the surface film is not interrupted by plastic walls, barriers or outlets. In this apparatus, the air bubble floats against a hydrophilic roof, e.g., of a 1% agarose gel, by buoyancy. At the air–agarose interface, the water layer is thin but sufficiently thick to prevent adhesion of the bubble to the gel itself. Bubble volume is controlled by varying the pressure in the sample chamber. As bubble volume is reduced, the surface area is reduced and the surface tension of the surfactant film at the bubble surface falls. The bubble shape changes de-

pending on the surface tension from more spherical to an oval shape. For bubbles larger than about 5 mm in initial diameter, the bubble shape assumes a thin disk as the surface tension falls towards zero. For surface tensions less than 1 mN/m up to about 30 mN/m, bubbles as small as 4 μl in volume (2 mm diameter) may be used in a sample volume of about 40 μl . However, usually bubbles of about 200 μl in volume (~ 7 mm diameter) are used in a sample volume of 0.5 to 1.0 ml. Surfactant concentrations, expressed in total phospholipid per volume (mg/ml), can be used from as little as 50 $\mu\text{g/ml}$ to a maximum of 1–2 mg/ml for the large chamber, 10 mm in diameter, while for the small chamber, 5 mm in diameter, a maximum concentration of 3 mg/ml may be used. The maximum concentration is given by optical limitations, because surfactant suspensions become murky at higher concentrations.

Surface tension, area and volume are calculated from bubble height and diameter, from video images [22]. For precision and accuracy of the method, see Refs. [20,22]. If more elaborate imaging processing is available, then the axisymmetric drop shape analysis (ADSA-P) by Neumann and associates, originally published by Rotenberg et al. [23], can be used. ADSA-P is exceptionally accurate and very general, but one limitation is that it requires the measurement of at least 20 points defining the bubble perimeter for input into a complex iterative computation (for more information, see Ref. [24]). The captive bubble surfactometer can be used to construct quasi-static isotherms similar to those obtained in the Langmuir–Wilhelmy balance and surfactant films can be compressed and expanded dynamically with cycling frequencies from extremely low to more than 100 cycles per minute.

3.2. Measurements of adsorption

Adsorption from a bulk surfactant suspension is generally measured by the rate of surface tension reduction (see above). If the relation between the amount (mass) of the accumulated surfactant (the surfactant concentration) in the surface (mass/unit area) and the surface tension is known, then the adsorption rate can be expressed in ($\mu\text{g cm}^{-2} \text{s}^{-1}$).

In the captive bubble surfactometer (CBS), two methods of bubble formation in a well-stirred surfac-

tant subphase have been used for the measurement of adsorption. In the first method, a small bubble, 2–3 mm in diameter, is introduced into the chambers of 10 mm in diameter with a small plastic tubing connected to a 50- μ l gas-tight microsyringe. The bubble is then expanded within a small fraction of a second by at least 10-fold in area by a sudden decrease in pressure either by reducing the pressure directly in the pressure-driven version of the captive bubble [25] or by increasing the chamber volume by the relative motion of the piston in the glass cylinder in the CBS version which employs volume changes to expand or compress the captive bubble [21]. The initial amount of surfactant on the bubble surface before expansion has to be taken into account for the exact analysis of the adsorption rate [26].

In the second approach, a bubble of a given volume of 200 μ l, approximately 7 mm in diameter, is formed through a 20-gauge needle positioned in the bottom inlet of the bubble chamber. In this method, the time interval for bubble formation is between 0.10 and 0.15 s, the time for 3–4 frames on the TV monitor. Again, the amount of surfactant accumulated on the bubble surface during bubble formation has to be determined for an exact analysis of the adsorption rate [26].

3.3. Surface activity of surfactants

A number of novel insights into surface properties have been obtained with the captive bubble. Adsorption from the stirred subphase proceeds rapidly with natural and organic solvent lipid extract surfactants, with equilibrium surface tensions of 23–25 mN/m being achieved in seconds with bulk concentrations at and above 1 mg/ml. With this method, reliable information about the mechanisms related to adsorption, film stability, hysteresis, and compressibility are obtained. For example, the mode of bubble cycling and the extent of film compression and collapse determine various amounts of hysteresis in surface tension–area relations obtained with lipid extract surfactants with or without added surfactant protein A (SP-A) [27,28]. In addition, detailed knowledge has been obtained from well-defined phospholipid dispersions with and without added surfactant-specific proteins [2].

3.3.1. Adsorption and film quality

As stated above, adsorption means the accumulation of material at an interface. An effective pulmonary surfactant adsorbs rapidly to form a film within a few seconds to around 25 mN/m, the plateau or equilibrium surface tension at the air–liquid interface [29]. Rapid adsorption toward equilibrium means that adsorption will keep the surface tension in the lung near equilibrium during inspiration to total lung capacity. This keeps the surface component of lung recoil pressure as low as possible, which helps to minimize the work of breathing [29]. In addition, low surface tension is important in maintaining the gas exchange area in the lung as large as possible and mechanically stable [30]. For lipid extract surfactants and natural lung surfactant extract, the plateau or equilibrium surface tension is between 23 and 25 mN/m at 37°C for concentrations above about 50 μ g/ml of total phospholipids [28]. The rate of adsorption is strongly dependent on the concentration of the lipid in the bulk suspension and whether SP-A is added to low-concentration lipid extract surfactant [27]. In general, rapid adsorption appears to be followed by low film compressibility and near zero and stable minimum surface tensions on quasi-static or dynamic compressions [28]. For example, bovine lipid extract (BLES) samples at 200 μ g/ml of phospholipid required more than 30 s to reach the equilibrium surface tension of approximately 25 mN/m after rapid expansion of the surface area. The amount of film area compression required from 25 mN/m to reach a minimum surface tension of 1 mN/m was 30% upon the first quasi-static compression [1,27]. In contrast, samples of 1 mg/ml required less than 5 s to reach equilibrium, and the film area compression required to achieve a minimum tension of 1 mN/m was only about 20%.

It appears that not only the level of the equilibrium surface tension (approximately 25 mN/m) but also the rate of film formation or the time interval required to reach that equilibrium value is important for the film quality. Such observations led to the conclusion that films which demonstrate low compressibility, close to that of pure DPPC films (~ 0.005 (mN/m)⁻¹) are being enriched in DPPC during the adsorption process [28].

Recent work on adsorption [28] demonstrates that fresh lipid extract surfactants that contain SP-B and

SP-C have the capacity to adsorb by a cooperative movement of large collective units of molecules into the interface during adsorption. The phenomenon of adsorption by the transport of lipid aggregates has been discussed previously [31]. In contrast to the clicks that characterize a sudden increase in surface tension accompanied by a decrease in surface area [21], the sudden adsorption bursts caused by the movement of lipid aggregates into the interface have been called adsorption clicks [28]. Adsorption related to the sudden movement of surfactant aggregates into the interface can easily be followed by the captive bubble technique. For example, for a large bubble of approximately 7 mm in diameter and a surface tension of 40 mN/m, a sudden change in surface tension to 35 mN/m is seen on the TV monitor as instantaneous large upward movement (click) of the bubble apex. A large adsorption burst, seen as ‘click’, may cause a decrease in the bubble surface tension of 10 mN/m in the first 0.1 s of the adsorption interval. This may result in the bubble surface tension reaching its plateau value of 23–25 mN/m in less than 0.1 s. Adsorption clicks are characterized by a stepwise decrease in surface tension of 5–10 mN/m corresponding to the incorporation of aggregates of up to 10^{14} phospholipid molecules into the interface. This phenomenon does not depend on the surface-associated protein SP-A, because lipid extract surfactants contain SP-B and SP-C but not SP-A. Furthermore, these adsorption clicks cannot be related to

tubular myelin, because these structures contain SP-A. Without exception, films formed in this manner appear already highly enriched in DPPC as seen by the extremely low compressibility close to that of DPPC. In contrast, films formed by gradual adsorption during several seconds to minutes may or may not show the same low compressibility as those formed by adsorption bursts. These latter films may then be purified by squeezing-out mechanisms [32].

Fig. 3 demonstrates both gradual slow adsorption to the equilibrium surface tension of approximately 25 mN/m and very rapid adsorption by adsorption bursts, seen as clicks of the captive bubble, from a low concentration (50 $\mu\text{g/ml}$) porcine lipid extract surfactant suspension.

Fig. 4 shows that the film area compressions required to reach near zero minimum surface tension were relatively high, 68% upon the first compression, 54% upon the second and 34% upon the third compression. High compressibility plateaus below 20 mN/m are evident for the first two compressions. These three isotherms demonstrate progressive purification with progressive cycling. In contrast, adsorption by adsorption bursts (Fig. 3) are followed by a very low compressibility film as seen by the low film area compression required, approximately 18%, upon the first quasi-static compression. Thus, the film formed by the adsorption by large collective units appears highly enriched in DPPC, as seen by the low compressibility of $0.010 \text{ (mN/m)}^{-1}$ at 15 mN/m which is close to that of a pure DPPC, $0.005 \text{ (mN/m)}^{-1}$ [28].

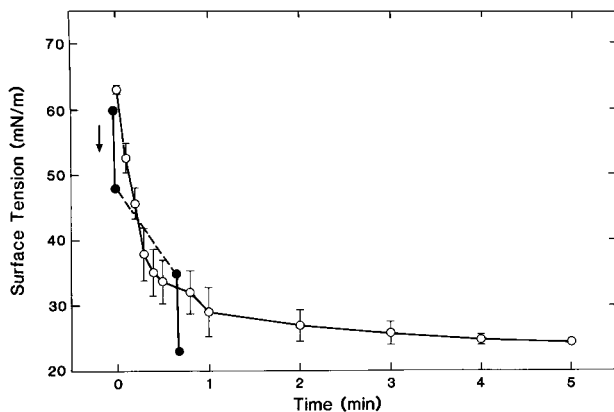


Fig. 3. Time course for adsorption of porcine lipid extract surfactant extract (Curosurf) at 50 $\mu\text{g/ml}$, for gradual adsorption (mean \pm S.E.M., $n=4$) (\circ). Typical adsorption in two sudden adsorption bursts (adsorption clicks) (\bullet). (From Schürch et al. [28], with permission.)

3.3.2. Film modifications during dynamic cycling

The Langmuir–Wilhelmy surface balance was introduced by Clements in 1957 [33] to investigate surfactant films in his pioneering studies on lung surfactant. With the Langmuir–Wilhelmy method, films from lung surfactant extracts are generally compressed to a fixed residual area of 50% to 10% of the initial area. This manner of film compression has frequently led to large hysteresis areas in the surface tension vs. area relations. The mechanisms involved in the hysteresis of these relations have been the subject of many investigations too numerous to be mentioned in detail. Hysteresis phenomena related to pulmonary surfactant have been discussed in several review articles [31,34,10].

We have used the captive bubble surfactometer to investigate the interrelated film properties that are involved in quasi-static or dynamic surface tension area relations [20,28]. Quasi-static cycling involves a series of small discrete alterations in bubble area where the surface film is allowed to ‘relax’ during the compression–expansion process. With dynamic cycling, in which the bubble volume is continuously altered at 20–30 cycles per minute (cpm), there is less opportunity for adsorption during the expansion phase and a greater possibility of overcompression (collapse at minimum tension) during the compression phase for given volume changes of the bubble.

The characteristics of dynamic surface tension–area loops, including maximum and minimum surface tension, film compressibility at surface tensions below about 25 mN/m, are largely related to the rate of film formation under dynamic conditions. Film reformation upon expansion in dynamically cycled films may involve the incorporation of material squeezed out during compression in the high compressibility range of surface tensions below about 25 mN/m and especially also from collapse material formed if films are compressed beyond the point where minimum surface tension is reached. This has been called overcompression [28] and is typical for surface tension–area loops conducted *in vitro* when films are compressed to a fixed residual area as in most Langmuir–Wilhelmy studies. The greater the film compressibility below 25 mN/m and the greater the overcompression at minimum surface tension, at near zero tensions for normal surfactant films, the greater is the hysteresis area of the surface tension–area loops. This hysteresis area represents the irreversible heat loss in the cycle.

Large hysteresis areas are thus typical for *in vitro* studies of surfactant extracts but also for particular pressure–volume studies on excised lungs, when the lungs are inflated from pressures below that corresponding to functional residual capacity or 40% of total lung capacity (TLC) [35]. Morphometric studies in conjunction with direct surface tension measurements by Bachofen and his associates [35] have demonstrated that surface tension–area hysteresis in excised rabbit lungs inflated from 40% TLC approaches zero especially if the lungs are ventilated between about 40 and 80% TLC. The change of the surface area measured in these lungs from 40% TLC

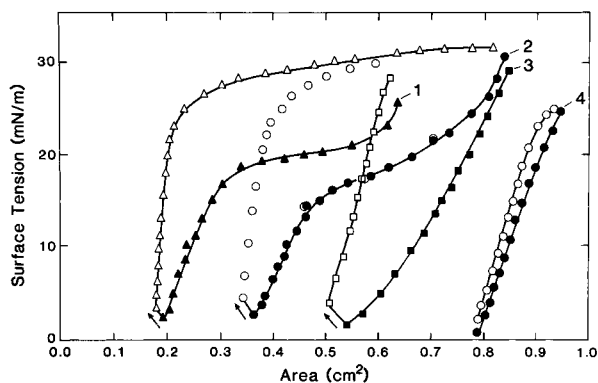


Fig. 4. Quasi-static isotherms of porcine lipid extract surfactant (Curosurf) Surface tension is plotted vs. bubble area for Curosurf at 50 $\mu\text{g}/\text{ml}$ during compression (filled symbols) and expansion (open symbols). Three typical consecutive isotherms after gradual adsorption (Nos. 1, 2, 3). Typical isotherms after adsorption by sudden adsorption bursts or adsorption clicks (No. 4). Note hysteresis and plateaus at a surface tension between 15 and 20 mN/m in isotherm Nos. 1 and 2. No hysteresis in isotherm No. 4 and film area compression to minimum surface tension approximately 16%, indicating film enriched in DPPC.

to TLC was approximately 30% [35]. This value is likely an overestimation as the preparation of the lungs for electron microscopy removes the aqueous subphase in the crevices of the crumpling air–blood barrier in the alveoli. Thus, the normal lung compresses its surface film, even for maximum volume excursions, much less than *in vitro* studies in the Langmuir–Wilhelmy balance (50–80%) or in the pulsating bubble surfactometer ($\sim 50\%$). Whereas overcompression at near zero minimum surface tension likely does not occur in the normal lung for normal tidal breathing, it may be a different matter when the surfactant is compromised by inhibitory agents, e.g., blood and serum proteins, or when the lung is mechanically ventilated. *In vitro* studies on inhibition demonstrate that the compressibility of surfactant films damaged by inhibitory agents tends to strive towards infinity or, in other words, the ‘squeeze-out plateaus’ tend to become horizontal. Recovery studies on optimizing surface activity in the captive bubble surfactometer show that film compression should be stopped once minimum surface tension is achieved, regardless of the level of minimum surface tension. Minimum surface tension is achieved when the height of the bubble is no longer reduced upon volume reduction, i.e., only the width of the bubble

decreases at the point of minimum surface tension. The surface activity of dynamically cycled films from damaged surfactant may be optimized by starting cycling with small volume excursions, corresponding to not more than about 20% film area changes, and by slowly increasing the volume excursions, but by avoiding overcompressions at minimum surface tension, whatever that value might be. Minimum surface tension is seen when the bubble height no longer decreases on its compression while the bubble diameter continues to shrink. Thus, ‘overcompression’ is redefined as compressions beyond the point at which minimum surface tensions are attained, regardless of the level of that minimum surface tension.

Fig. 5 demonstrates the effect of phospholipid concentration on the shape of loops from dynamically cycled films from bovine lipid extract surfactant in the presence and absence of SP-A. The initial total film area compressions were approximately 50% of the initial bubble area. In Fig. 5B,C, the area changes to obtain near zero surface tension for the stationary loops remained 28–30%; in contrast, the loops in Fig. 5A show that more than 80% film area reduction was required to obtain near zero minimum surface tension for the stationary loops centering on cycle 20. The lipid extract surfactant (BLES) concentration in Fig. 5A was 0.2 mg/ml. In Fig. 5C, BLES was 0.2 mg/ml supplemented with 4% (w/w) SP-A. In Fig. 5B, BLES was at 1.0 mg/ml. Thus, stationary loops with moderate film area compressions to near zero surface tensions are obtained with surfactant either at a substantially higher concentration than that for Fig. 5A or when the low surfactant concentration is supplemented by SP-A [27].

A number of interesting features can be observed at low surfactant concentrations (0.2 mg/ml BLES). During dynamic compressions with low BLES concentrations, a distinct plateau occurs below 25 mN/m where a decrease in surface area of 30% results in only a small reduction in surface tension. Previous studies with the Langmuir–Wilhelmy balance have termed this phenomenon the ‘purification’ or ‘squeeze-out’ plateau, because it appears as though non-DPPC lipids are being removed as opposed to simple packing of monolayer lipids, which would result in the reduction of surface tension below the equilibrium tension of 25 mN/m (e.g., Ref. [31]). It has been suggested that squeeze-out corresponds to

the exclusion of the lipid-expanded phase, and an increase in the percentage of condensed DPPC domains resulting in a partial enrichment in DPPC [32]. However, recent experiments have demonstrated that films from porcine lipid extract surfactant exhibit no plateau upon area compression, a very low film compressibility, close to that of pure DPPC films (~ 0.005 m/mN) after de novo adsorption, and near zero and stable surface tensions after a moderate area compression between 15% and 20% [28].

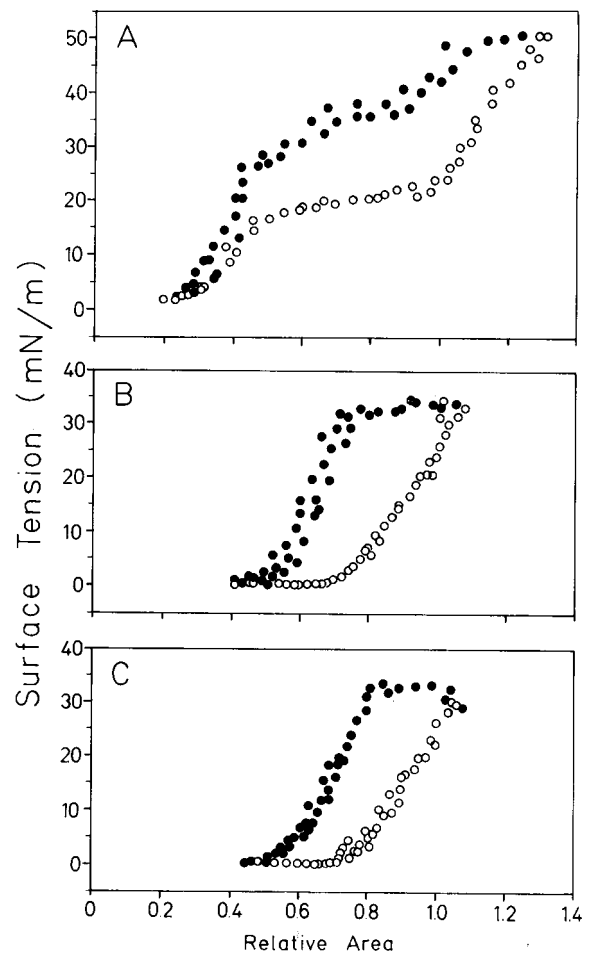


Fig. 5. Effect of concentration and SP-A on dynamic hysteresis loops of lipid extract surfactant (BLES). Surface tension is plotted versus relative area. Plots are the summaries of four consecutive dynamic cycles centering on the 20th cycle. Open symbols indicate measurements made during compression; filled symbols indicate measurements made during expansion. Samples were suspended in 0.9% NaCl, 1.5 mM CaCl₂. A, BLES at 200 μ g/ml; B, BLES at 1000 μ g/ml; C, BLES at 200 μ g/ml, supplemented with 4% SP-A. (Adapted from Schürch et al. [27], with permission.)

Yet, when these films were cycled dynamically with overcompression at near zero minimum surface tension, a distinct plateau was generated which was clearly related to collapses at near zero surface tension. There appear to be several mechanisms involved in plateau formation in the compression part of a dynamic surface tension–area cycle, including squeeze-out and film collapse at near zero surface tension. Both mechanisms are important in the overall film surface activity.

Another feature of the dynamic cycles at low concentration of BLES is a shoulder above 35 mN/m in the expansion portion of the curve (Fig. 5A). This shoulder is considered due to adsorption from a distinct pool of lipids referred to as the ‘surface reservoir’ [1,27] because adsorption from the bulk suspension at low lipid concentration is too slow to explain the relatively rapid adsorption that causes the shoulder. In addition there was a delay in the rise of surface tension, clearly seen in Fig. 5B,C, at the start of film expansion. This feature is not consistent with the characteristics of monolayer expansion [27].

To clarify the mechanisms involved in the formation of the characteristic features of the hysteresis loop, such as those observed in Fig. 5A at low lipid concentrations in the bulk phase, we have reduced the bulk lipid concentration to zero by depleting the subphase of surfactant after the initial film formation by adsorption. By this approach phenomena related to the ‘reservoir’ can clearly be distinguished from those related to the bulk surfactant phase.

4. The surface-associated surfactant reservoir

Depletion experiments with the captive bubble system have demonstrated the presence of ‘surplus’ material in the air–liquid interface generated upon de novo adsorption of surfactant derived from natural sources. The material in excess of a monolayer has been termed ‘the surface-associated surfactant reservoir’ [1]. For lipid extract surfactants (BLES and Curosurf), there was a surplus of material equivalent of at least two monolayers associated with the surface or material for a total of at least three monolayers after adsorption to 23–25 mN/m [1,10]. In this section, we will discuss the surfactant film surface activity including adsorption, compressibility, mini-

mum surface tension and mechanical stability. These parameters will be related to the surfactant reservoir.

4.1. Reservoir formation: the role of SP-B and SP-C

To obtain insight into potential mechanisms involved in the formation of the surface-associated reservoir and the incorporation (adsorption) of material from this reservoir into the surface active film, depletion studies were conducted with a lipid mixture containing the major surfactant phospholipids, DPPC and PG 7:3 by weight, dispersed in 0.9% NaCl, 1.5 mM CaCl₂, pH 6.0. Several differences were noted between the properties of the DPPC/PG 7:3 and the lipid extract surfactants BLES and Curosurf. First, whereas the lipid extract surfactants achieved equilibrium surface tensions in seconds by adsorption, the lipid mixtures reached a plateau at a surface tension of 34 mN/m in 5 min. This difference can be attributed to the ability of the low-molecular-mass hydrophobic proteins SP-B and SP-C to enhance sur-

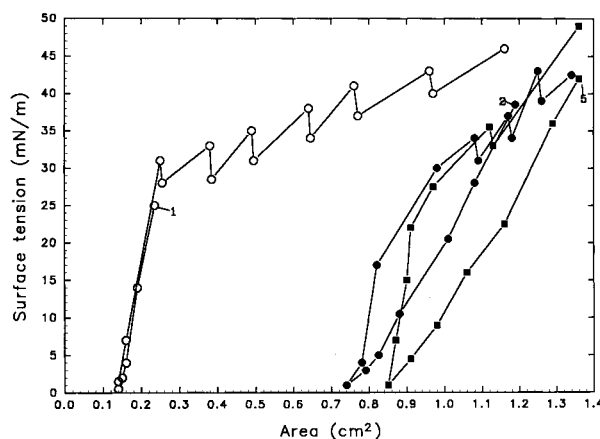


Fig. 6. Subphase depletion after film formation in DPPC/PG=7:3 by weight, pH 6.5 in 0.9% NaCl+1.5 mM CaCl₂+1% SP-C. Series of five consecutive quasi-static compression–dynamic expansion cycles conducted at increasing bubble areas in the captive bubble surfactometer after subphase replacement with the pure salt solution. Numbers (1, 2, 5) indicate start of film compressions. Peaks represent relatively high surface tensions generated by stepwise, rapid area expansions. Each peak is followed by a decrease in surface tension by adsorption of material from the ‘surface-associated surfactant reservoir’. The film area at minimum surface tension after the fifth quasi-static compression indicates the existence of surfactant material after de novo adsorption equivalent to six monolayers. Film area compressions from 25 to 0.5 mN/m for all of the cycles between 37% and 43%.

face film formation. Furthermore, to attain surface tensions near zero, the area of the surface film derived from the lipid mixture had to be reduced by about 80% during the first compression from 34 mN/m and by approximately 70% for the following compressions from 34 mN/m, indicating only a slight enrichment in DPPC under these conditions. In contrast, films formed from lipid extract surfactants at equilibrium require only a 20% reduction in surface area to achieve surface tensions of 1–2 mN/m upon the first quasi-static compression. Hence, these films behave as if they were highly enriched in DPPC. The fact that similar film area compressions for lipid extract surfactant are sufficient to reduce the surface tension to low values in subsequent compressions from larger surface areas indicates that the material incorporated from the surface-associated reservoir does not modify the initial film structure. Finally, in contrast to the lipid extract surfactants in which enriched surface active material corresponding to several monolayers could be incorporated into the surface film, only material equivalent to approximately half a monolayer could be incorporated from the surface-associated reservoir of the mixed films without the surfactant proteins.

The suggestion that the low-molecular-mass hydrophobic surfactant apoproteins could be involved in the formation of the surface reservoir led to reconstitution studies involving SP-B and SP-C. Depletion experiments revealed that when SP-B (1%, w/w) was added to DPPC/PG 7:3, an area reduction of only 28% was sufficient to lower the surface tension from equilibrium (25 mN/m) to less than 1.0 mN/m during the first compression. Similar area reductions resulted in surface tensions near zero after bubble expansion and the film compressibility at 15 mN/m remained approximately $0.010 \text{ (mN/m)}^{-1}$. Excess material equivalent to approximately two monolayers could be incorporated into the surface active film. Reconstitution studies with the captive bubble surfactometer involving DPPC/PG 7:3 samples containing SP-C (1%, w/w) showed that an area reduction of more than 35% was required to achieve surface tensions near zero mN/m with the first and subsequent compressions. This value was intermediate between the value of 80% observed with DPPC/PG 7:3 alone and the 28% observed with DPPC/PG 7:3 containing 1% SP-B. The film compressibilities at

15 mN/m were approximately 0.17 (mN/m)^{-1} for the five compressions. Depletion experiments showed that when SP-C (1%, w/w) was added to DPPC/PG 7:3, excess material equivalent to approximately five additional monolayers could be incorporated into the surface active film (Fig. 6).

These studies are consistent with the concept that both SP-B and SP-C contribute to alveolar stability, but that these hydrophobic proteins contribute distinct properties to the alveolar lining layer. SP-B ap-

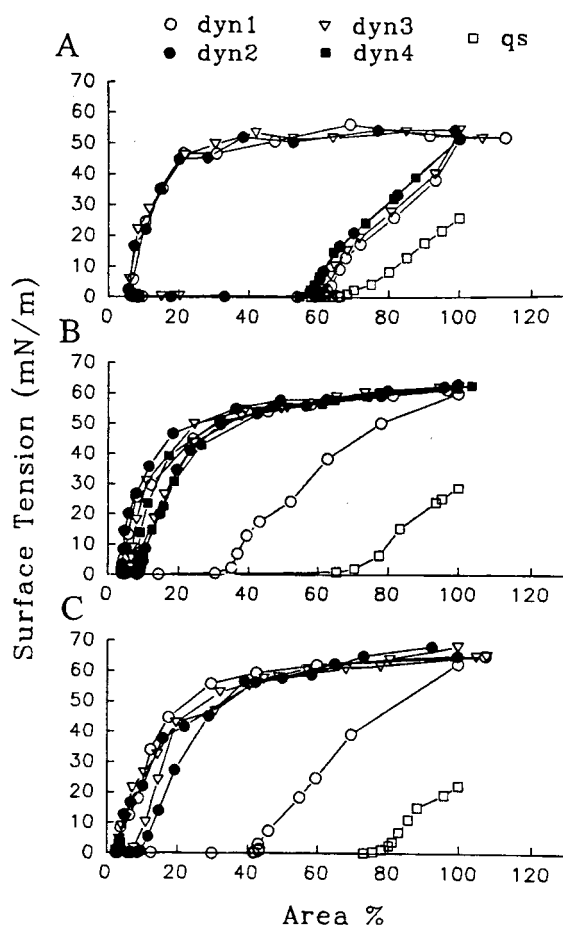


Fig. 7. Subphase lipid depletion. The first quasi-static isotherm (qs) and subsequent dynamic cycles (dyn 1–4) after the depletion of surfactant in the subphase are depicted for DPPC-PG-palmitoylated SP-C (A), DPPC-PG-depalmitoylated SP-C (B), and DPPC-PG-SP-B (C). Quasi-static compression produced $< 5\%$ collapse. During dynamic cycling, however, all samples were overcompressed, giving a final area compression of 90–95%. The first point of the first dynamic cycle follows the last point in the quasi-static curve. Data are representative of six experiments. (From Qanbar et al. [2], with permission.)

pears to be more effective than SP-C in enhancing selective adsorption of DPPC, whereas SP-C appears to be more effective in promoting incorporation of additional material from the surface reservoir into the surface active film. In addition, SP-C appears to enhance the mechanical stability of pulmonary surfactant films at near zero minimum surface tension to a greater extent than SP-B. This is supported by the recent results of Qanbar and co-workers [2], who demonstrated that mixed films of DPPC and PG possessed greater mechanical stability in the presence of SP-C than when formed in the presence of SP-B. The studies of Qanbar et al. also showed that SP-C palmitoylation dramatically increases film stability of mixed phospholipid films in contrast to the depalmitoylated form of SP-C which induced film instability, as seen by increased bubble clicking at near zero surface tensions. In addition, palmitoylation plays an important role in film recovery after film collapse at near zero minimum surface tension. This is demonstrated in Fig. 7. Palmitoylated SP-C promoted the total incorporation of the collapse material into the surface active film in a series of successive dynamic cycles with film area compressions of approximately 80%. This mechanism could neither be matched by SP-B nor by depalmitoylated SP-C.

These depletion experiments serve to explain the characteristics of surface tension–area relations obtained from dynamically compressed and expanded captive bubbles in suspensions of phospholipid mixtures when either SP-B or SP-C was added (Figs. 8 and 9). The tracings of the dynamic cycles (20–30 cpm) obtained from suspensions with SP-B show a maximum surface tension of approximately 60 mN/m, whereas the maximum tension from the SP-C containing samples was about 50 mN/m. This reflects a greater capacity of SP-C compared to SP-B for reforming dynamically compressed films. However, the film compressibility at 15 mN/m was lower in the presence of SP-B than in the presence of SP-C, 0.010 vs. 0.015 (mNm)⁻¹, respectively. This appears to be in line with the results of Yu and Possmayer [36] who found that SP-B was not as effective as SP-C in enhancing phospholipid adsorption but was more effective in enriching the films with DPPC. However, whether SP-B or SP-C is more effective in enhancing adsorption appears to depend on the

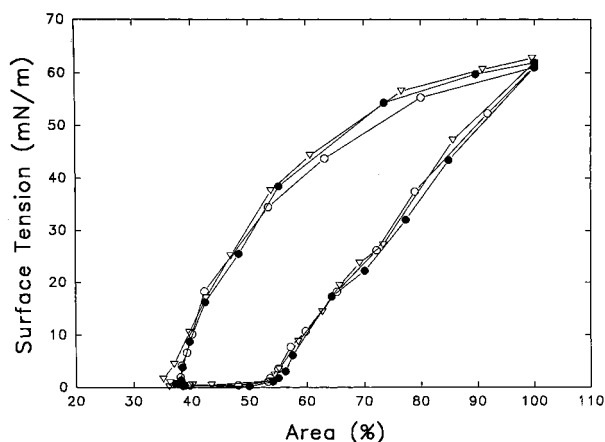


Fig. 8. Dynamic compression–expansion cycles. Cycles 19 (○), 20 (●) and 21 (▽) of 30 consecutive cycles are plotted for DPPC/PG, 7:3 by weight+1% SP-B.

conditions used. For example, Wang and co-workers [37] consistently found that SP-B was more effective than SP-C in facilitating lipid adsorption and in the ability to lower surface tension to near zero values. These studies on film recovery implied that SP-B and SP-C were similar in their ability to increase re-spreading in dynamically cycled films in the Langmuir–Wilhelmy balance. However, the films in the surface balance were formed by spreading from surfactant dissolved in a solution of hexane and ethanol. In contrast, the studies on film recovery in the captive bubble were conducted on adsorbed films after subphase depletion. Since differing methods have

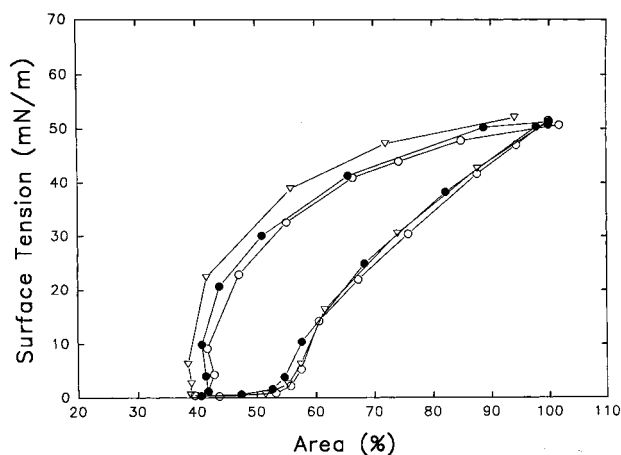


Fig. 9. Dynamic compression–expansion cycles. Cycles 19 (○), 20 (●) and 21 (▽) of 30 consecutive cycles are plotted for DPPC/PG, 7:3 by weight +1% SP-C.

been employed by various investigators, it is not surprising that differing results are found.

It is interesting to note that, in our reconstitution studies with DPPC/PG 7:3 (w/w) with either 1% SP-B or 1% SP-C added, the dynamic cycles were substantially different from those obtained from lipid extract surfactant (Fig. 5C), although the phospholipid concentration was the same (1 mg/ml) in both studies. Adsorption under dynamic conditions seems to be more efficient for lipid extract surfactant than for the lipid mixtures. It is not certain whether the combination of both proteins, SP-B and SP-C, or other lipid components are responsible for the greater efficiency in the dynamic adsorption behavior of lipid extract surfactant.

In summary, the surfactant-associated proteins SP-B and SP-C enhance the surfactant film formation by promoting selective adsorption of DPPC and/or squeeze-out of components other than DPPC upon film compression. SP-B appears more effective than SP-C for selective adsorption, whereas SP-C is more effective than SP-B for film reformation from a collapse phase and in stabilizing mechanically the surfactant film at near zero minimum surface tension.

5. Film structure

5.1. Alveolar surface lining layer

Illustrations in textbooks of physiology attribute to the alveolar lining layer the following structural properties: (1) it is a continuous duplex layer consisting of an aqueous hypophase covered by a thin surfactant film; (2) the surfactant film is a monolayer with dipalmitoyl-phosphatidylcholine (DPPC) as most important component; (3) the surface film is stable in the lung volume range of normal breathing.

There are numerous studies of the structure of the lining layer, all of which are fragmentary. Indeed, the preservation and sample preparation of this delicate structure for microscopy is extremely difficult; there is no standard to distinguish between facts and artifacts, and it is not readily conceivable of how monolayers of saturated phospholipids can be preserved and visualized by the usual fixatives [38]. As to the first postulate, i.e., the existence and continuity of a duplex layer, Weibel and Gil were the first to convincingly demonstrate a two-phase lining layer by transmission electron microscopy (e.g., Ref. [5]). They found a hypophase of variable thickness and

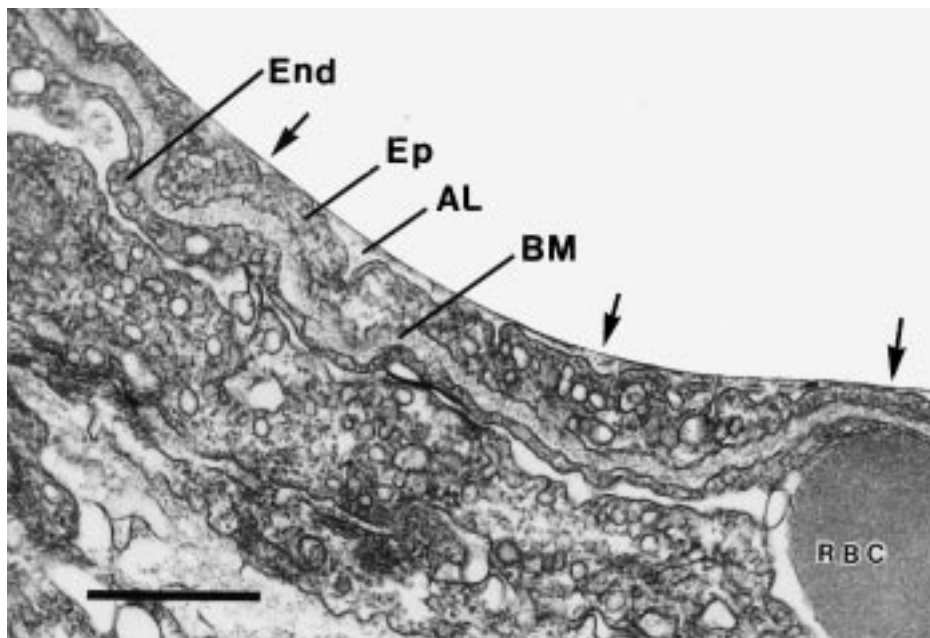


Fig. 10. Transmission electron micrograph from guinea pig lung after fixation with non-aqueous osmium fluorocarbon mixture. The surfactant film (arrows) is preserved and continuous and overlies a thin hypophase which is thicker at some sites (AL) above the type I epithelium (Ep). End, endothelial cell; BM, basement membrane. Bar = 0.5 μ m.

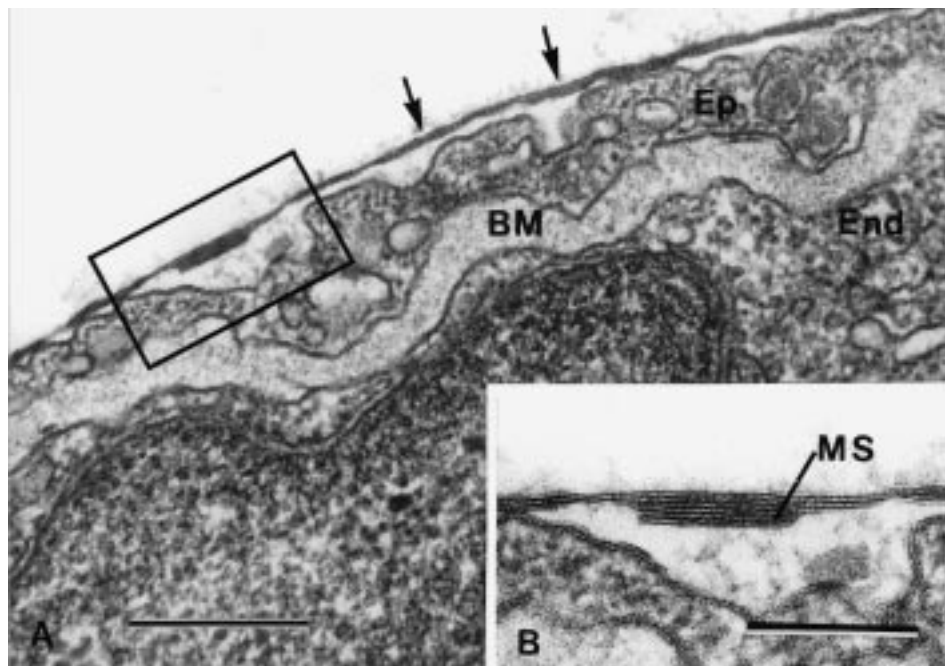


Fig. 11. (A) Higher magnification of the alveolar surface film from a guinea pig lung showing that it is multilaminated. Bar = 0.3 μm . (B) Close-up of alveolar surface film over type I pneumocyte showing variations in the number of lamellae from 2 to 7. A multilamellar structure (MS) resembling a disk-like vesicle is partially incorporated into the surface film. Bar = 0.6 μm .

composition which could best be recognized in the numerous depressions of the epithelial surface, and, in alveolar corners. The surface film appeared as osmiophilic layer at sites where the hypophase was clearly visible. However, the film was often fragmented and disposed in patches, and could not be detected on flat parts of the alveolar walls. Although studies of freeze-fractured preparations suggested its continuity [39], the exact structure of the lining layer in situ remained a matter of debate. Quite recently, however, Bastacky et al. [8] clearly demonstrated the continuity of the aqueous lining layer by low-temperature electron microscopy: it varies from a few nanometers to several micrometers in thickness such that surfactant can be absorbed and spread over the entire surface. Improved tissue preparations in conjunction with perfusion fixation [9] resulted also in a better visualization of the surfactant film such that all evidence available suggests a continuum of the duplex layer.

As to the second postulate, i.e., a monolayer as surface film, the structural evidence is rather scanty. Already the micrographs of Weibel and Gil [5] and Ueda et al. [7] as well as more recent high-power

magnifications of the film revealed a rather polymorphous structure [10]. At some sites, the surface film appears to be an amorphous material, at other sites, triple layers or even multilayers can be recognized, and quite generally it appears to be thicker than a monolayer of phospholipids. Certainly, the latter finding might be an artifact caused by the heavy metals used as staining material.

As to the third postulate, i.e., film stability at lower lung volumes, the structural findings are not revealing so far. However, microscopic observations of alveolar microdroplets show extremely slow increases in the surface tension and minimal γ - V hysteresis within the volume-range of normal breathing, thus giving indirect evidence of a stable surface film.

5.2. Multilayers at the alveolar surface

As the precise structure of the film is still in question, the search for improved fixation techniques have continued. Sims et al. [40] and others [41] have used a non-aqueous fixation technique to preserve mucus in bovine, guinea pig and rat trachea. The technique involves dissolving osmium tetroxide

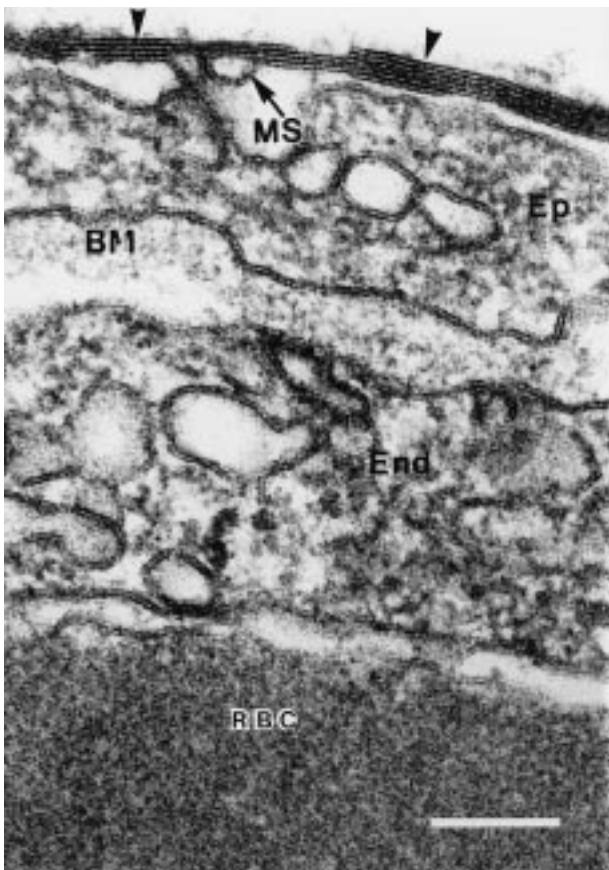


Fig. 12. Alveolar surface film over type I pneumocyte at thin air–blood barrier. A multilamellar structure (MS) is partially incorporated into the surface film. Bar = 0.1 μm .

in a non-aqueous perfluorocarbon fluid (FC) with the aim of stabilizing mucus glycoprotein and glycosaminoglycan molecules, as well as phospholipids in the surfactant material, before dilution in aqueous fixation can occur.

Recent investigations on the alveolar film structure, after fixation by instillation of the non-aqueous medium of osmium tetroxide dissolved in perfluorocarbon, have demonstrated a continuous film covering the entire alveolar surface, including the pores of Kohn. By transmission electron microscopy (TEM), the surface film frequently appears multilayered [42]. Fig. 10 shows that the surfactant film is preserved and continuous, and overlies a thin hypophase above type I epithelial cells. At higher magnification (Fig. 11A,B) the surface film appears to be multilaminated with variation in the number of lamellae from 2 to 7. In addition, the high magnification boxed area (Fig. 11B) shows a multilaminated structure, its main

body appears planar. The structure is closed at the right-hand side but open at the left-hand side, as if the bent layers seen at the left had broken off. This certainly might be an artifact. The structure appears disk-like attached to the film consisting of planar lamellae. Fig. 12 depicts the structure of the thin air–blood barrier of an alveolus. Again, the surfactant film is multilaminated. A multilayer structure (MS) appears partially integrated into the multilamellar surface film, consisting of 4–7 straight lamellae.

5.3. Surface film *in vitro*: recent investigations

5.3.1. Fluorescence, Brewster angle and scanning force microscopy

We refer to Chapter II by Possmayer and his associates and especially to the Chapter IX by Pérez-Gil and Keough for the recent quantitative studies on the organization of surfactant lipids and proteins at the air–water interface, using epifluorescence and Brewster angle microscopy. In fluorescence light microscopy, mixed surfactant lipid monolayers formed in the presence of SP-B or SP-C or both appear to be phase separated. Such studies have shown that both SP-B and SP-C can remain associated with DPPC monolayers under various stages of dynamic compression. Both proteins occupy the liquid expanded (LE) phase and appear to increase the LE phase relative to the more ordered condensed phase. At low surface tensions, mixed phospholipid films containing DPPC were enriched with DPPC as seen through the relatively high amounts of condensed phase formed in such films.

Amrein and his associates [43,44] have used scanning force microscopy to investigate Langmuir–Blodgett films formed from spread monolayers of DPPC, DPPG and SP-C. The spread films showed a plateau above the surface pressure of 50 mN/m (below a surface tension at 22 mN/m) where film material was reversibly removed from the monolayer but remained associated with it. The scanning force microscopy showed the reversible formation of laminated protrusions upon compression. These protrusions consist of stacks of lipid double layers, containing SP-C, consistent with the concept of the surface-associated reservoir formed upon film compression. In view of these findings, we might interpret the

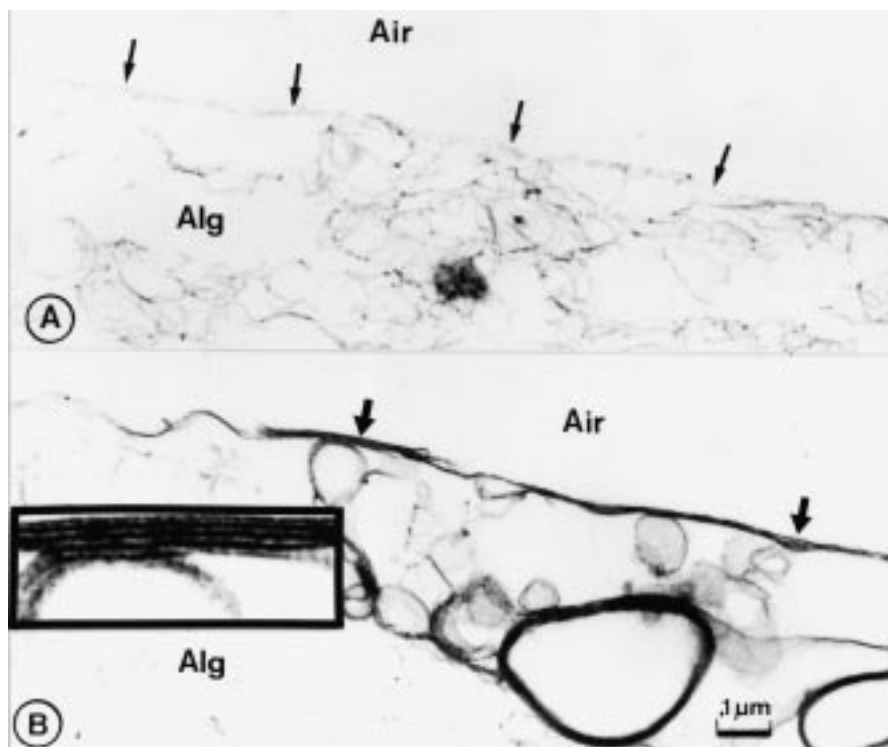


Fig. 13. Surfactant films of captive bubbles fixed with non-aqueous osmium fluorocarbon fixative. (A) Faint and fragmented surfactant films (arrows) are seen if the alginate solution contained 0.3 mg/ml lipid extract surfactant (Curosurf). (B) Conspicuous film formation is seen with suspensions at higher concentration (1 mg/ml) with frequent multilayers (arrows). Boxed area: multilaminated film below arrow in B, but at four times higher magnification. Air, air of captive bubble; Alg, solidified alginate solution.

structural organization of the multilaminated films seen on our electron micrographs as stacks of bilayers forming a reservoir associated with the surface active film (see above).

5.3.2. Electron microscopy

Few attempts have been made to study the structure–function relationship of surface films *in vitro* by electron microscopy and, in particular, at different points of compression–expansion isotherms. The reason for this lack of experimental data is that the fixation of an extremely fragile surface film together with an undisturbed layer of aqueous hypophase to preserve the molecular arrangements is a seemingly impossible task.

Reiss and collaborators [45] succeeded in transferring pieces of surfactant film from the surface balance to coated coppergrid for shadow casting and analysis with the electron microscope. At low degree of film compression, they found an irregular pattern of islands separated by open spaces. At high com-

pression, that is, at low surface tensions, only inhomogeneous collapsed films with highly irregular areas could be observed.

More recently, a new attempt has been made to analyze the structure–function relationship of the surface film of bubbles in a ‘captive bubble surfactometer’ [46]. The usual aqueous surfactant suspension (from which surfactant is adsorbed to the surface of the bubble) is replaced by an alginate surfactant suspension. Control experiments have shown that the alginate solution does not interfere with the function of surfactant. By addition of calcium, the alginate solution is solidified together with the bubble and its surface without a detectable change of shape and size. The block is then fixed, cut, and processed for electron microscopy. Some preliminary findings are noteworthy. (1) With a surfactant suspension of low concentration (0.3 mg lipid extract surfactant in 1 ml of alginate solution), only a faint, amorphous and fragmented film can be visualized at the bubble surface (Fig. 13A), although the

behavior of the bubble before solidification of its hypophase demonstrated clear-cut surface activity. (2) With suspensions of high concentration (1 mg/ml), a more distinct and continuous film is formed at the bubble surface. Remarkably, this film was formed without the addition of SP-A to the lipid extract surfactant. The film is of variable thickness, and multilayer formations are frequent (see Fig. 13B). So far, one can only speculate about these findings and more research is needed, but it is tempting to suggest that the good surface activity seen in dynamically cycled films formed from 1 mg/ml lipid extract surfactant at 1 mg/ml (Fig. 5C) is related to the multilaminated structure.

6. The surfactant film: monolayer or multilayer?

6.1. Film structure

The alveolar surface film frequently seems to be multilaminated, not only in alveolar corners and crevices, but also at the thin air–blood barrier above the capillaries. Disk-like structures (Fig. 11B) or multilamellar vesicles (Fig. 12) appear attached or partially integrated into the planar multilayered film. Frequently, there is an odd number of laminae, but at some sites the film facing the air phase appears to be a bilayer or to have an even number of laminae. So far, the existence of a monolayer could not be demonstrated by electron microscopy.

As stated above, the fixation of a monofilm is likely very difficult, if not impossible, with the present fixation techniques. So, if we see three laminae, the film might consist of a monolayer with an attached bilayer, or if we see seven laminae, there might be a stack of three bilayers with a monolayer on top facing the air phase. However, the spacing between two adjacent laminae always seems to be between 4 and 5 nm, so assuming the top lamina is a monolayer, it could not be distinguished from the stack of bilayers by examining the spacing. If the film appears to consist of an even number of laminae, then the top layer facing the air phase might be missing because it had not been sufficiently stabilized by the chemical fixation. From the point of view of traditional concepts, one would certainly argue against the existence of a bilayer film facing the air

phase. However, it is noteworthy that Gershfeld and co-workers [47,48] described the spontaneous formation of lecithin surface films, which can exceed monolayer concentrations. The existence of a new, bilayer phase which was first deduced from thermodynamic arguments was supported by experimental evidence [48]. However, the formation of a surface bilayer appears to depend on the presence of a liquid-crystal phase in the bulk suspension [47,48].

6.2. Film formation

The surfactant mesophase in the aqueous layer consists of a variety of molecular aggregates including unilamellar and multilamellar vesicles and the well-known tubular myelin structures. Film formation seems to occur from tubular myelin directly or from vesicles. Multilayer formation at the air–water interface at the surface of a captive bubble (Fig. 13) does not depend on the presence of SP-A as seen in their formations *in vitro* from lipid extract surfactant.

Williams et al. [49] described the generation of discoidal (disk-like) particles formed by stacked bilayers by the combination of surfactant lipids with SP-B and SP-C or with SP-B alone. The multilamellar structure (MS) in Fig. 11B might be such a stacked bilayer form and seems to be a part of the multilaminated film. The structural properties of SP-B and SP-C have been extensively studied by Johansson and Curstedt [50] and others (see the preceding chapters by Hawgood, Johansson and Weaver).

SP-B is built up of several amphipathic helices due to charged amino acids throughout its sequence. The hydrophobic character is due to leucine, valine and isoleucine in one of the helices. The α -helices interact preferentially with superficial parts of the phospholipid bilayers [51]. When present in a surface film, SP-B more efficiently promotes lipid insertion from subphase vesicles than does SP-C [52]. SP-B may cross-link two phospholipid bilayers to form multilayered structures and due to its fusion promoting properties may generate planar multilamellar structures at the air–liquid interface, consistent with the film structure seen in electron micrographs (Figs. 11–13). SP-C contains a 3.7 nm long α -helix with a 2.6 nm long very hydrophobic poly-valyl part. The SP-C α -helix is oriented in a transmembrane way in a phospho-

lipid bilayer where the poly-valyl helical part interacts with the fatty acid chains [53]. The entire transmembrane helix is needed for the surface activity of surfactant. SP-C and synthetic analogs having transmembrane orientation appears to promote spreading and adsorption of an air–water interface more efficiently than the amphipathic SP-B and synthetic amphipathic peptides (see chapter by Johansson). Furthermore, surfactant lipid mixtures which contain SP-C are mechanically more stable than those containing SP-B.

In summary, both SP-B and SP-C promote lipid adsorption and spreading *de novo* at an air–water interface, but SP-C appears to be more efficient than SP-B [50]. SP-B more efficiently promotes lipid insertion from surface-associated vesicles or multilamellar structures than does SP-C. Yet, this mechanism seems to depend on the way the surface-associated structures are generated. If the structures are formed by film collapse, they probably contain less water than the ‘unmanipulated’ aggregates in the subphase. In this case, SP-C appears to be more efficient for the reformation of the film upon dynamic surface expansion (Fig. 7). Both SP-B and SP-C are closely associated with the surfactant bilayer or multilayered aggregates in the subphase with different helical orientation and location, and both proteins are also part of the surface film after its formation at the air–water interface. Rapid film formation implies that, in association with the lipid aggregates in the aqueous solution, the hydrophobic sites of both SP-B and SP-C increase the free energy of the aggregates to a value above that which the lipid vesicles would have without the proteins. At the air–water interface, the lipid–protein association may spontaneously assume a configuration which minimizes the free energy that is the hydrophobic sites and moieties face the air phase. Thus, the adsorption process is accompanied by a substantial decrease in the free energy, such that the rate of surfactant accumulation is enhanced in spite of an energy barrier due to the work needed to clear surface area against the surface pressure (see Eq. 4 in Section 2.2.2).

6.3. Monolayer hypothesis

In the traditional, widely accepted view, the lining

layer of surfactant should be composed of two parts, a monomolecular film of phospholipids with partially integrated (SP-B, SP-C) and the partially associated specific surfactant protein (SP-A) and an aqueous subphase. The air–bulk liquid interfacial tension is determined by the monolayer surface tension.

6.4. Monolayer approximation

According to previous work mentioned above and more recent studies, using improved fixation techniques, including fixation by a non-aqueous medium, the alveolar air–water film is multilaminated or amorphous, but it always appears to be thicker than the cell membrane of a type I cell. Electron micrographs of the surfaces of air bubbles within a lipid extract surfactant suspension (captive bubbles) disclosed complex structures of the surface film. In particular, at high lipid extract concentrations of the suspensions, multilayered films became visible. The morphological findings are in line with *in vitro* depletion experiments using the captive bubble method, showing that surfactant material associated with the interface can be incorporated into the surface active film upon dynamic bubble expansion. The surfactant layer facing the air may be free to slide relative to the adjacent laminae, that is the top layer and the layers below are uncoupled and would not develop mechanical moments due to changes of curvature [54]. For this situation, the monolayer approximation can be used, that is the shape of the interfacial area is consistent with a Laplacian shape, as discussed below.

6.5. Surface tension: mechanical equilibrium

The tension between the vapor phase and the bulk liquid phase in the lung is lowered by the presence of a film at the vapor–liquid interface. The most general interface separating a liquid and a gas or two immiscible liquids will have, at any point, a maximum and a minimum radius of curvature R_1 and R_2 , respectively. These are the principal radii of curvature and occur in planes that are perpendicular to each other, and are both perpendicular to the tangent plane to the surface. The Laplace equation of capillarity relates the pressure difference P across the in-

terface at any point to the radii of curvature at the point by

$$P = \gamma(1/R_1 + 1/R_2)$$

where γ is the surface tension for the liquid–gas interface, or the interfacial tension for a fluid–fluid interface [11]. The shape of such an interface, even if it is modified by a monolayer or a thin film, is denoted ‘Laplacian’ if the equation above applies to any point of the interface. The Laplace equation describes the equilibrium of the mechanical forces within the interface, even though the system as a whole is often in a thermodynamically nonequilibrium state.

Our use of the term ‘surface tension’ follows the theory of Ono and Kondo [55] and of Defay and Prigogin [56]. Thus, we use ‘surface tension’ for the vapor–water interfacial tension for any surfactant film whose shape is ‘Laplacian’.

To test whether the shape, for example, of a captive bubble is ‘Laplacian’, the approach by Neumann and associates as originally published by Rotenberg et al. can be employed [23]. This axisymmetric drop shape analysis (ADSA) has been adapted to many experimental situations [24].

6.6. Nonmonolayer properties

The time-dependent response of film or membrane deformation to applied forces is determined by the rate of viscous dissipation in the material. This viscoelastic behavior does not involve irrecoverable (plastic) material deformation [54]. The following observations on surfactant films are not consistent with the concept of a monolayer or of a multilayered film in mechanical equilibrium, although the films might be characterized by a ‘local mechanical equilibrium’ [54].

1. There is a small delay in surface tension upon area expansion in dynamically cycled films of lipid extract surfactant, compressed beyond the area at which near zero minimum surface tension is obtained (overcompression) (see Fig. 5).
2. Surfactant-associated proteins substantially decreased film compressibility of mixed phospholipid films and modify their structure such that the bubble shape at surface tensions below 1 mN/m

clearly starts to deviate from a Laplacian shape. This is especially noticeable for films with SP-C.

3. Lipid extract films and phospholipid mixtures with added SP-B and/or SP-C compressed to low surface tension are mechanically far more stable than phospholipid monolayers, DPPC, or mixtures of DPPC and PG in the absence of SP-B or SP-C. The films with added SP-B and/or SP-C can tolerate mechanical disturbances and revert to the undisturbed original bubble shape in a time-dependent manner at low minimum surface tensions. The bubbles with spread phospholipid monolayers always revert spontaneously and rapidly to higher surface tensions (bubble clicks) upon mechanical deformation by stir bar action in the captive bubble chamber.

7. Summary and future directions

There is ‘surplus’ surfactant material in excess of a monolayer at the air–liquid interface upon de novo adsorption of surfactants derived from natural sources or of phospholipid mixtures with added SP-B and/or SP-C. This ‘surface-associated reservoir’ is larger when SP-A is added to SP-B and/or SP-C. In addition to the reservoir formed by de novo adsorption, an additional reservoir is formed during film compression, especially if the films are compressed beyond the point where minimum surface tension is obtained regardless of the level of minimum surface tension. The mode of area extension or cycling in vitro and possibly the mode of ventilation of lungs can be chosen such that the surface-associated material can be incorporated into the surface active film. Although the surfactant film seems to be too thick to be a monolayer and frequently appears to be multilayered, the Laplacian shape of the interfaces in the captive bubble system is consistent with the shape of an interface modified by a monolayer.

The deviation of the bubbles from a Laplacian shape at very low surface tension in combination with the depletion experiments and the morphological observations in situ and in vitro suggest that the surfactant film cannot be considered a simple monomolecular layer.

There is no doubt that future experiments will be

directed toward the structural analysis of the surfactant film and toward the role of the surfactant-associated proteins in the three-dimensional organization of the surfactant lipids. The knowledge with regard to the film architecture is also relevant for the understanding of the inhibitory action of blood proteins. We believe that the film structure, its surface activity and resistance to mechanical disturbances, and inhibitory action of blood proteins are determined not only by the biochemical composition of the film, but also by its architecture after de novo adsorption and by structural modification resulting from the mode of cycling.

8. List of Symbols

| | |
|------------|--|
| $c(x,t)$ | Concentration at location x and time t (e.g., kmol m ⁻³) |
| c_0 | Initial concentration of bulk solution |
| D | Diffusion coefficient (m ² s ⁻¹) |
| Γ | Surface concentration (kmol m ⁻²) |
| Γ_e | Equilibrium surface concentration |
| k | Boltzmann constant (1.380662×10^{-23} J K ⁻¹) |
| Π | Surface pressure |

Acknowledgements

This work was supported by the Medical Research Council of Canada, the Alberta Heritage Foundation for Medical Research, and the Swiss National Science Foundation. We thank BLES Biochemicals Inc., London, Ontario, for the lipid extract surfactant BLES. The authors wish to thank Dr. John A. Clements for his pioneering work and for his many original contributions toward exploring the interesting area of the lung's surfactant system. One of the authors (S.S.) is very grateful for having had the opportunity to work in John Clement's laboratory and to measure the surface tension directly in the alveoli of the lung.

References

- [1] S. Schürch, R. Qanbar, H. Bachofen, F. Possmayer, The surface associated surfactant reservoir in the alveolar lining, *Biol. Neonate* 67, (suppl. 1) (1995) 61–76.
- [2] R. Qanbar, S. Cheng, F. Possmayer, S. Schürch, The role of the palmitoylation of surfactant-associated protein C in surfactant film formation and stability, *Am. J. Physiol.* 271 (1996) L572–L580. *Lung Cell Mol. Physiol.* 15
- [3] R.E. Pattle, Surface tension and the lining of the lung alveoli, in: C.G. Caro (Ed.), *Advances in Respiratory Physiology*, Edward Arnold Ltd., London, 1966.
- [4] M.H. Klaus, J.A. Clements, R.J. Havel, Composition of surface-active material isolated from beef lung, *Proc. Natl. Acad. Sci. U.S.A.* 47 (1961) 1858–1859.
- [5] E.R. Weibel, J. Gil, Electron microscope demonstration of an extracellular lining layer of alveoli, *Respir. Physiol.* 4 (1968) 42–57.
- [6] G. Grossmann, B. Robertson, Lung expansion and the formation of the alveolar lining layer in the full-term newborn rabbit, *Acta Paediatr. Scand.* 64 (1975) 7–16.
- [7] S. Ueda, N. Ishii, S. Masumoto, K. Hayashi, M. Okayasu, Ultrastructural studies on surface lining layer of the lungs. Part II, *Jpn. Med. Soci. Biol. Interface* 14 (1983) 30–35.
- [8] J. Bastacky, C.Y.C. Lee, J. Goerke, H. Koushafar, D. Yager, L. Kenaga, T.P. Speed, Y. Chen, J.A. Clements, Alveolar lining layer is thin and continuous: low-temperature scanning electron microscopy of rat lung, *J. Appl. Physiol.* 79 (1995) 1615–1628.
- [9] H. Bachofen, S. Schürch, R.P. Michel, E.R. Weibel, Experimental hydrostatic pulmonary edema in rabbit lungs: morphology, *Am. Rev. Respir. Dis.* 147 (1993) 989–996.
- [10] S. Schürch, H. Bachofen, Biophysical aspects in the design of therapeutic surfactant, in: B. Robertson, H.W. Taeusch (Eds.), *Surfactant Therapy for Lung Disease* (In series: C. Lenfant (Ed.), *Lung Biology in Health and Disease*), Marcel Dekker, New York, 1995, pp. 3–32.
- [11] A.W. Adamson, *Physical Chemistry of Surfaces*, 5th ed., John Wiley, New York, 1990, pp. 1–777.
- [12] D.K. Chattoraj, K.S. Birdi, *Adsorption and the Gibbs Surface Excess*, Plenum, New York, 1984, pp. 1–471.
- [13] N.K. Adam, *The Physics and Chemistry of Surfaces*, Republication of 3rd ed. 1941, Dover, New York, 1968.
- [14] C.-H. Chang, E.I. Franses, Adsorption dynamics of surfactants at the air/water interface: a critical review of mathematical models, data, and mechanisms, *Colloids Surfaces* 100 (1995) 1–45.
- [15] J.D. Andrade (Ed.), *Principles of Protein Adsorption in Surface and Interfacial Aspects of Biomedical Polymers*, vol. 2, Protein Adsorption, Plenum, New York, 1985, pp. 1–80.
- [16] J.T. Davies, E.K. Rideal, *Interfacial Phenomena*, 2nd ed., Academic, New York, 1962.
- [17] S. Damodaran, K.B. Song, Adsorption of proteins at the air–water interface: role of protein conformation, in: K.L. Mittal (Ed.), *Surfactants in Solution* vol. 8, Plenum, New York, 1989, pp. 391–410.
- [18] R. Becker, *Theorie der Wärme*, Springer, Berlin, 1964, pp. 1–320.
- [19] A. Pacault, *Éléments de Thermodynamique Statistique*, Masson, Paris, 1963, pp. 1–358.
- [20] S. Schürch, H. Bachofen, J. Goerke, F. Possmayer, A cap-

- tive bubble method reproduces the in situ behavior of lung surfactant monolayers, *J. Appl. Physiol.* 67 (1992) 2389–2396.
- [21] S. Schürch, H. Bachofen, J. Goerke, F.H.Y. Green, Surface properties of rat pulmonary surfactant studied with the captive bubble method: adsorption, hysteresis, stability, *Biochim. Biophys. Acta* 1103 (1992) 127–136.
- [22] W.M. Schoel, S. Schürch, J. Goerke, The captive bubble method for the evaluation of pulmonary surfactant: surface tension, area and volume calculations, *Biochim. Biophys. Acta.* 1200 (1994) 281–290.
- [23] Y.L. Rotenberg, L. Boruvka, A.W. Neumann, Determination of surface tension and contact angle from the shapes of axisymmetric fluid interfaces, *J. Colloid Interface Sci.* 93 (1983) 169–183.
- [24] F.K. Skinner, Y. Rotenberg, A.W. Neumann, Contact angle measurement from the contact diameter of sessile drops by means of a modified axisymmetric drop shape analysis, *J. Colloid Interface Sci.* 130 (1989) 25–34.
- [25] G. Putz, J. Goerke, S. Schürch, J.A. Clements, Evaluation of pressure-driven captive bubble surfactometer, *J. Appl. Physiol.* 76 (1994) 1417–1424.
- [26] G. Putz, J. Goerke, J.A. Clements, Surface activity of rabbit pulmonary surfactant subfractions to different concentrations in a captive bubble, *J. Appl. Physiol.* 77 (1994) 597–605.
- [27] S. Schürch, F. Possmayer, S. Cheng, A.M. Cockshutt, Pulmonary SP-A enhances adsorption and appears to induce surface sorting of lipid extract surfactant, *Am. J. Physiol.* 263 (1992) L210–L218.
- [28] S. Schürch, D. Schürch, T. Curstedt, B. Robertson, Surface activity of lipid extract surfactant in relation to film area compression and collapse, *J. Appl. Physiol.* 77 (1994) 974–986.
- [29] J. Goerke, J.A. Clements, Alveolar surface tension and lung surfactant, in: *Handbook of Physiology, The Respiratory System Mechanics of Breathing*, vol. III, part 1, American Physiological Society, Bethesda, MD, 1986, pp. 247–261.
- [30] H. Bachofen, S. Schürch, F. Possmayer, Disturbance of alveolar lining layer: effects on alveolar microstructures, *J. Appl. Physiol.* 76 (1994) 1983–1992.
- [31] K.M.W. Keough, Physical chemistry of pulmonary surfactant, in: B. Robertson, L.M.G. van Golde, J.J. Batenburg (Eds.), *The Terminal Airspaces*, Elsevier, Amsterdam, 1992, pp. 109–164.
- [32] A. Boonman, F.H.J. Machiels, A.F.M. Snik, J. Egberts, Squeeze-out from mixed monolayers of dipalmitoyl phosphatidylcholine and egg phosphatidylglycerol, *J. Colloid Interface Sci.* 120 (1987) 456–468.
- [33] J.A. Clements, Surface tension of lung extracts, *Proc. Soc. Exp. Biol. Med.* 95 (1957) 170–172.
- [34] R.H. Notter, Surface chemistry of pulmonary surfactant: the role of individual components, in: B. Robertson, L.M.G. van Golde, J.J. Batenburg (Eds.), *Pulmonary Surfactant*, Elsevier, Amsterdam, 1984, pp. 17–65.
- [35] H. Bachofen, S. Schürch, M. Urbinelli, E.R. Weibel, Relations among alveolar surface tension, surface area, volume and recoil pressure, *J. Appl. Physiol.* 62 (1987) 1878–1887.
- [36] S.-H. Yu, F. Possmayer, Role of bovine pulmonary surfactant-associated proteins in the surface active property of phospholipid mixtures, *Biochim. Biophys. Acta* 1046 (1990) 233–241.
- [37] Z. Wang, O. Gurel, J.E. Baatz, R.B. Notter, Acylation of pulmonary surfactant protein-C is required for its optimal surface active interactions with phospholipids, *J. Biol. Chem.* 271 (1996) 19104–19109.
- [38] G.B. Dermer, The fixation of pulmonary surfactant for electron microscopy, *J. Ultrastruct. Res.* 27 (1969) 88–104.
- [39] P. Untersee, J. Gil, E.R. Weibel, Visualization of extracellular lining layer of lung alveoli by freeze etching, *Respir. Physiol.* 13 (1971) 171–185.
- [40] D.E. Sims, J.A. Westfall, A.L. Kiorpes, M.M. Horne, Preservation of tracheal mucus by nonaqueous fixative, *Biotech. Histochem.* 66 (1991) 173–180.
- [41] M.M. Lee, S. Schürch, S.H. Roth, X. Jiang, S. Cheng, S. Bjarnason, F.H.Y. Green, Effects of acid aerosol exposure on the surface properties of airway mucus, *Exp. Lung Res.* 21 (1995) 835–851.
- [42] F.H.Y. Green, P. Gehr, M.M. Lee, S. Schürch, Particle lung interactions: surfactant, in: C. Lenfant (Ed.), *Lung Biology in Health and Disease*, 1997, in press.
- [43] M. Amrein, A. von Nahmen, M.A. Sieber, Scanning force- and fluorescence light microscopy study of the structure and function of a model pulmonary surfactant, *Eur. Biophys. J.* 26 (1997) 349–357.
- [44] A. von Nahmen, M. Schenk, M. Sieber, M. Amrein, The structure of a model pulmonary surfactant as revealed by scanning force microscopy, *Biophys. J.* 72 (1997) 463–469.
- [45] O.K. Reiss, G.W. Paul, J. Gil, An electron microscopic study of thin films of alveolar surfactants and dipalmitoyl phosphatidylcholine: film collapse at high surface pressures, *Prog. Respir. Res.* 18 (1984) 29–35.
- [46] S. Schürch, H. Bachofen, Alveolar lining layer: functions, composition, structures, in: M.P. Hlastala, H.T. Robertson (Eds.), *Complexities in Structure and Function of the Lung* (In series: C. Lenfant (Ed.), *Lung Biology in Health and Disease*), Chapter 2, Marcel Dekker, New York, 1998, pp. 35–73.
- [47] N.L. Gershfeld, K. Tajima, Spontaneous formation of lecithin bilayers at the air–water surface, *Nature* 279 (1979) 708–709.
- [48] K. Tajima, N.L. Gershfeld, Phospholipid surface bilayers at the air–water interface. I. Thermodynamic properties, *Biophys. J.* 47 (1985) 203–209.
- [49] M.C. Williams, S. Hawgood, R.L. Hamilton, Changes in lipid structure produced by surfactant proteins SP-A, SP-B and SP-C, *Am. J. Respir. Cell Mol. Biol.* 5 (1991) 41–50.
- [50] J. Johansson, T. Curstedt, Molecular structures and interactions of pulmonary surfactant components, *Eur. J. Biochem.* 244 (1997) 675–695.
- [51] M.R. Morrow, J. Pérez-Gil, G. Simatos, C. Boland, J. Stew-

- art, D. Absolom, V. Sarin, K.M.W. Keough, Pulmonary surfactant-associated protein SP-B has little effect on acyl chains in dipalmitoylphosphatidylcholine dispersions, *Biochemistry* 32 (1993) 4397–4402.
- [52] M.A. Oosterlaken-Dijksterhuis, H.P. Haagsman, L.M.G. van Golde, R.A. Demel, Interaction of lipid vesicles with monomolecular layers containing lung surfactant proteins SP-B or SP-C, *Biochemistry* 30 (1991) 8276–8281.
- [53] J. Johansson, G. Nilsson, R. Strömberg, B. Robertson, H. Jörnvall, T. Curstedt, Secondary structure and biophysical activity of synthetic analogues of the pulmonary surfactant polypeptide SP-C, *Biochem. J.* 307 (1995) 535–541.
- [54] E.A. Evans, R. Skalak, *Mechanics and Thermodynamics of Biomembranes*, CRC Press, Boca Raton, FL, 1980, pp. 1–254.
- [55] S. Ono, S. Kondo, Molecular theory of surface tension in liquids, in: S. Flügge (Ed.), *Encyclopedia of Physics*, Springer, Berlin, 1960, pp. 134–280.
- [56] R. Defay, I. Prigogine, *Surface Tension and Adsorption*, John Wiley, New York, 1966.